Journal of the Chinese Society of Mechanical Engineers, Vol.47, No.1, pp105~114 (2026)

Optimizations of Friction Stir Welding Parameters of AA6061-T6 and AA7075-T6 Aluminum Alloys

İbrahim Ülke*, Mustafa Yurdakul** and Yusuf Tansel İç***

Keywords : aluminum alloy, response surface methodology, friction stir welding, optimization, factorial design.

ABSTRACT

In our study, the effects of test parameters on the weld quality in friction stir butt welding of AA7075-T6 and AA6061-T6 aluminum alloy sheets, each with a thickness of 2 mm and dimensions of 125 mm x 100 mm, are examined. Three different control variables, each with three levels, tool inclination angle 1°, 0.5 °, and 0°, tool rotation speed 1000 rpm, 710 rpm, and 500 rpm, tool feed rate 40 mm/min, 28 mm/min, and 20 mm/min were applied. The experiments are carried out to weld AA6061-AA7075, AA7075-AA7075, and AA6061-AA6061 pairs, consisting of two different aluminum material plates using the Box-Behnken experimental design. Each experiment is performed three times (three replications). The output analysis of the experiments is provided in this paper.

INTRODUCTION

Studies on friction stir welding are generally aimed at optimizing the process parameters and improving the welding process. The friction stir welding process includes various control variables for permanently joining plates of AA6061-T6 and AA7075-T6. Aluminum alloys are preferred, especially in the aviation industry, because of their high machinability values, low purchase prices, and densities. Although there are various studies in this area in the literature, studies that combine analysis of the experiments' results with optimization, development of equations that link input (control) variables with the output (response) variables, and obtaining an overall single objective function are limited.

Paper Received November, 2022. Revised January, 2025. Accepted January, 2025. Author for Correspondence: Yusuf Tansel İç.

* *MSc, Department of Mechanical Engineering, Gazi University, Ankara, 06570, Turkiye.*
** *Prof. Dr., Department of Mechanical Engineering, Gazi University, Ankara, 06570, Turkiye.*
** *Prof. Dr., Department of Industrial Engineering, Baskent University, Ankara, 06790, Turkiye*

LITERATURE REVIEW

Applications of friction stir welding (FSW) are available in the literature. Sahu et al. (2021) investigated the effects of tool feed rate, tool rotational speed, and tool geometry for friction stir welding 5083-aluminum alloy material plates. Harisha et al. (2022) investigated the effects of tool feed rate and tool rotation speed on tensile strength when combining copper and 6083 series aluminum alloys with FSW. Chowdhury et al. (2022) investigated the effects of ultrasonic vibrations applied at 10, 12, and 14 kHz frequencies on surface hardness and tensile strength considering tool feed rate and tool rotation speed for the combination of C26000 copper alloy and 6063 aluminum alloy with FSW. Shekar et al. (2022) investigated the effects of tool feed rate and ultrasonic vibrations on 6013 and 6063 series aluminum alloys. Wu et al. (2021) analyzed the effects of tool feed rate and tool materials in the joining of 5A06 and 2A70 aluminum alloys with FSW. Yaghoubi and Shirazi (2021) studied the effects of tool feed rate and tool rotation speed in joining copper plates with FSW. Singh (2021), MirHashemi et al. (2021), Rahmatian et al. (2020), and Moradi et al. (2019) investigated the effect of nanoparticles with different properties added to the weld area on the weld quality when joining various aluminum alloy materials with FSW. Kumar et al. (2021), Sun and Fujii (2015), Fathi et al. (2019), and Liu et al. (2013) conducted studies on the optimization of the process parameters for friction stir welding of plates made of 6061 aluminum alloy. Shunmugasundaram et al. (2020) 6063 and 5052 series, Thilagham and Muthukumaran (2020) 6082 and 7075 series, Khan (2020) 6062 series, and Maneiah et al. (2020) performed an optimization study for 6061 series aluminum alloys. Verma and Kumar (2021) welded dissimilar plates made of AA6061-T6 and AA5083-O with the FSW type. Sandeep et al. (2021) optimized the process parameters of the FSW process to maximize the mechanical properties of the AA6082/B4C composite weldments using a genetic algorithm and desirability function approach for aircraft wing structures. Pitchipoo et al. (2021) presented a multi-objective optimization methodology (Dragonfly Algorithm) to optimize the weld strength

of FSW of aluminum alloy 6082-T6. Balamurugan et al. (2021) proposed a study to examine the influence of process parameters on tensile strength and microstructural frame for two dissimilar aluminum alloys of AA5052-H32 and AA6061-T6. Banik et al. (2021) studied three different tool pin geometries for FSW of AA 6061-T6 to determine the best tool geometry that optimizes the final weld properties. Jia et al. (2021) analyzed the mechanical properties of welded joints for the FSW outcome quality. Prabhu et al. (2021) examined the AA 6061/TiO2 composites obtained with the FSW.

The FSW studies available in the literature generally applied to combinations of the same material. On the other hand, Ghiasvand et al. (2021) investigated the effects of tool offset on the mechanical properties of friction stir welded AA6061-T6 and AA7075-T6 plates. Mohammed et al. (2021) investigated the effect of process parameters and tool profiles on the tensile strength of AA6061-AA7075 joints. We analyzed the effects of tool feed rate, tool rotation speed, and tool tilt angle for the weldment of 6061 and 7075 series aluminum alloys with FSW. The three combinations studied in this study are 6061-6061, 6061-7075, and 7075-7075.

MATERIALS AND METHOD

Materials

In this study, 125 mm length × 100 mm width plates of AA6061-T6 and AA7075-T6 aluminum alloy materials are friction stir welded. The chemical compositions of the materials are provided in Table 1. Their mechanical properties are shown in Table 2. Before performing the welding tests, the plates were cut, rough edges were smoothed, and contact surfaces were cleaned with pure alcohol.

Tooling and Equipment

Selection of the proper rotating tool material is critical in FSW (Umanath et al. 2021). AISI H13 HSS (DIN 1.2344) hot work rotating tool steel is selected in this study (Figure 1). The shoulder diameter of the tool used in the study is 18 mm, the pin diameter is 4 mm, and the pin length is 1.7 mm. The tool geometry is designed as a straight cylinder.

Table 1. Chemical compositions of AA6061-T6, AA7075-T6 plates.

Mate-rials	Alloy elements (%)								
	Si	Cr	Mn	Mg	Cu	Ti	Fe	Zn	Al
AA6061-T6	0.4-0.8	0.04-0.35	0.00-0.15	0.8-1.2	0.15-0.40	0.00-0.15	0.0-0.7	0.00-0.25	Other
AA7075-T6	0.0-0.4	0.18-0.28	0.00-0.30	2.1-2.9	1.20-2.00	0.00-0.20	0.0-0.5	5.10-6.10	Other

Table 2. Mechanical properties of AA6061-T6, AA7075-T6 plates.

Materials	Yield Strength	Tensile Strength	Shear Strength	Elongation	Module of Elasticity	Melting Temperature
AA6061-T6	270 MPa	310 MPa	207 MPa	%15	69 GPa	582 °C
AA7075-T6	480 MPa	560 MPa	330 MPa	%8	71.7 GPa	466 °C

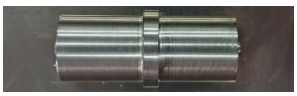

Fig. 1. Cylindrical tool set made of AISI H13 HSS material

Friction stir welding processes were performed on a right-headed universal milling machine with a rotation speed range of 500-1000 rpm, a feed rate range of 20-40 mm/min, and a tool tilt angle range of 0-1°. Six flat boots and one split pin with a support hole are used to fix the plates on the work table. After completion of the experiments, the weldment samples were left to cool in the air at room temperature. After cooling, the samples are cleaned and prepared for measurements.

METHODOLOGY

An overview of the previous FSW studies indicates that the four parameters that critically affect the quality of the weldment are tool geometry, tool feed rate, tool rotation speed, and tool tilt angle. Tool geometry is not included in the scope of this study since it contains many variables such as tool material, pin diameter, pin geometry, pin length, and shoulder diameter. The process parameters are determined based on previous studies. Tool rotation speed and feed rate values are obtained by considering the plate thicknesses and melting points. The mechanical properties and microstructures were investigated depending on the change in weld thickness with the tool tilt angle. In the study, the immersion depth is taken constant as 0.1 mm. The tool tilt angle is varied in this study as 0°, 0.5° and 1°. The levels of tool rotation speed and tool feed rate are determined approximately by using the mathematical equations provided in references (Rzaev et al. 2019; Gill et al. 2018). The optimum levels of control factors are obtained for three different combinations (Table 3), namely, AA6061-AA6061, AA7075-AA7075, and AA6061-AA7075 (Figure 2).

The factors that are kept constant in the study are shown in Table 4. An experiment plan is developed using the Box-Behnken response surface experimental design (Banik et al. 2021). Pictures of some of the experiments performed are presented in Figure 2, and the explanations of these pictures are presented in Table 5.

Table 3. Factors affecting the performance characteristics and their levels.

Code	Factors	Symbol	Unit	Level 1	Level 2	Level 3
A	Tool Rotation Speed	TRS	(rpm)	500	710	1000
B	Tool Feed Rate	TFR	(mm/ min)	20	28	40
C	Tool Tilt Angle	TTA	(°)	0	0,5	1

Table 4. Constant factors and their values.

Factor	Unit	Value
Plunge depth	mm	0.1
Waiting time for plunge	s	30
Speed for plunging	mm/min	14
Tool geometry	-	Cylinder
Tool diameter	mm	18
Pin diameter	mm	4
Pin length	mm	1.7

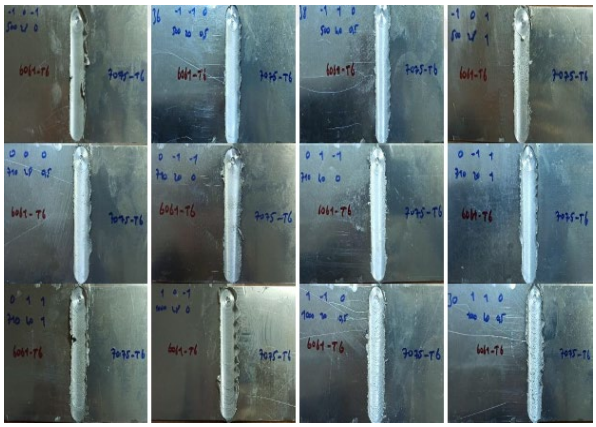

Fig. 2. Sample examples of weldments of aluminum alloy pair of AA6061-AA7075 plates.

FINDINGS

After the 135 pairs of plates are joined, a tensile test specimen is cut from each pair of plates with the water jet. Each sample's tensile strength and elongation values are recorded after the tensile tests (Table 6).

Optimization

In this section, a multi-objective optimization study to calculate optimal factor values that meet the two objectives' (the tensile strength and elongation) target values is presented. The response surface methodology is applied to obtain the two objective functions (regression equations). Regression equations represent the relationships between the input factors and responses.

Table 5. Explanation of sample examples in Figure 2.

Factor Levels: -1 0 -1 A: 500 rpm B: 28 mm/min C: 0°	Factor Levels: -1 -1 0 A: 500 rpm B: 20 mm/min C: 0.5°	Factor Levels: -1 1 0 A: 500 rpm B: 40 mm/min C: 0.5°	Factor Levels: -1 0 1 A: 500 rpm B: 28 mm/min C: 1°
Factor Levels: 0 0 0 A: 710 rpm B: 28 mm/min C: 0.5°	Factor Levels: 0 -1 -1 A: 710 rpm B: 20 mm/min C: 0°	Factor Levels: 0 1 -1 A: 710 rpm B: 40 mm/min C: 0°	Factor Levels: 0 -1 1 A: 710 rpm B: 20 mm/min C: 1°
Factor Levels: 0 1 1 A: 710 rpm B: 40 mm/min C: 1°	Factor Levels: 1 0 -1 A: 1000 rpm B: 28 mm/min C: 0°	Factor Levels: 1 -1 0 A: 1000 rpm B: 20 mm/min C: 0.5°	Factor Levels: 1 1 0 A: 1000 rpm B: 40 mm/min C: 0.5°

Table 6. Average tensile strength and average elongation values of the samples.

Tool Rotation Speed (rpm)	Tool Feed Rate (mm/min)	Tool Tilt Angle (°)	AA6061-AA6061		AA6061-AA7075		AA7075-AA7075	
			Average Tensile Strength (MPa)	Average Elongation (%)	Average Tensile Strength (MPa)	Average Elongation (%)	Average Tensile Strength (MPa)	Average Elongation (%)
500	20	0.5	156.1	5.8	161.8	4.0	201.0	1.5
1000	20	0.5	148.3	6.2	167.9	3.9	219.4	2.1
500	40	0.5	154.3	6.0	168.5	4.5	214.3	1.8
1000	40	0.5	163.2	4.2	175.7	4.4	216.0	2.3
500	28	0	150.0	4.7	173.4	4.5	212.2	1.9
1000	28	0	157.4	5.2	179.1	4.4	228.9	1.9
500	28	1	177.9	5.9	178.7	4.5	221.0	2.1
1000	28	1	166.0	5.1	184.9	3.5	226.3	2.7
710	20	0	133.3	5.4	177.7	3.7	190.2	2.6
710	40	0	134.8	6.0	160.0	5.0	177.9	2.2
710	20	1	150.0	6.3	168.7	4.8	189.3	3.7
710	40	1	169.2	5.5	184.4	5.6	214.1	2.8
710	28	0.5	148.5	6.1	167.0	5.0	208.0	2.8
710	28	0.5	164.2	4.1	165.9	4.6	210.9	2.6
710	28	0.5	146.9	4.5	169.1	4.3	212.6	2.6

The error (deviation) between the experiment results and the responses is measured with R-sq (adj) values. The deviation level must be lower than a pre-defined acceptable level for the acceptability of a regression equation. In this study, two acceptable regression equations are calculated for each combination of the material types (Table 7). As an example, it is observed that the tensile strength of the weldments increases when the tool rotation speed increases for the AA7075 aluminum alloy plates. On the other hand, tensile strength decreases for the weldments of the AA6061 alloy plates (Figure 3).

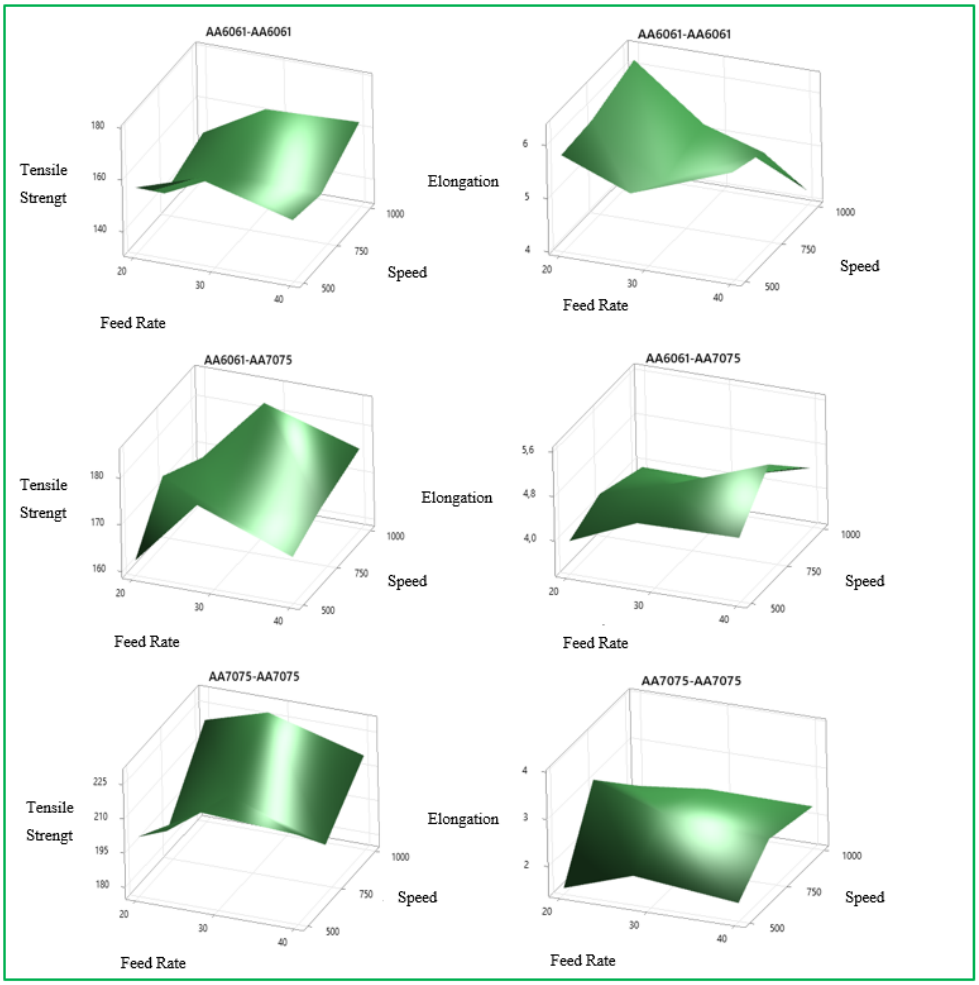

Fig. 3. Tensile strength and elongation output graphs.

After obtaining the regression equations, optimization is performed using the goal programming methodology in this study. Goal Programming methodology is a well-known and successful multi-objective optimization methodology (Yurdakul et al. 2022). Equations 1-10 provide the developed goal programming model using the regression equations along with the responses' target values and other constraints.

$$\text{Min } Z = +d_1^+ + d_2^+ + d_3^+ + d_4^- + d_5^- + d_6^- \quad (1)$$

Targets:

$$Y1_{\sigma_{max}AA6061-AA6061} = 155.2 - 0.2170\ x_1 + 4.77\ x_2 - 12.1\ x_3 + 0.000149\ x_1^2 - 0.0857\ x_2^2 + 5.82\ x_3^2 + 0.000068\ x_1{*}x_2 - 0.0215\ x_1{*}x_3 + 1.511\ x_2{*}x_3 + d_1^+ - d_1^- = 157 \quad (2)$$

$$Y2_{\sigma_{max}AA6061-AA7075} = 177.9 - 0.2048\ x_1 + 4.55\ x_2 - 27.4\ x_3 + 0.000149\ x_1^2 - 0.0857\ x_2^2 + 5.82\ x_3^2 + 0.000068\ x_1{*}x_2 - 0.0215\ x_1{*}x_3 + 1.511\ x_2{*}x_3 + d_2^+ - d_2^- = 175 \quad (3)$$

$$Y3_{\sigma_{max}AA7075-AA7075} = 167.4 - 0.2837\ x_1 + 9.32\ x_2 - 23.6\ x_3 + 0.000244\ x_1^2 - 0.1469\ x_2^2 - 16.72\ x_3^2\ \ 0.001651\ x_1{*}x_2 - 0.0258\ x_1{*}x_3 + 1.952\ x_2{*}x_3 + d_3^+ - d_3^- = 204 \quad (4)$$

$$Y4_{\sigma_{max}AA6061-AA6061} = 6.25 + 0.0055\ x_1 - 0.24\ x_2 + 3.22\ x_3 + 0.000149\ x_1^2 + 0.00703\ x_2^2 + 1.19\ x_3^2 - 0.000231\ x_1{*}x_2 - 0.00261\ x_1{*}x_3 - 0.0744\ x_2{*}x_3 + d_4^+ - d_4^- = 5 \quad (5)$$

$$Y5_{\sigma_{max}AA6061-AA7075} = +1.29 + 0.01171\ x_1 + 0.049\ x_2 + 1.79\ x_3 - 0.000007\ x_1^2 + 0.00001\ x_2^2 + 0.29\ x_3^2 - 0.000006\ x_1{*}x_2 - 0.00212\ x_1{*}x_3 - 0.0121\ x_2{*}x_3 + d_5^+ - d_5^- = 4 \quad (6)$$

$$Y6_{\sigma_{max}AA7075-AA7075} = -4.47 + 0.0182\ x_1 + 0.001\ x_2 - 0.17\ x_3 - 0.000012\ x_1^2 - 0.00011\ x_2^2 + 0.773\ x_3^2 + 0.000007\ x_1{*}x_2 + 0.00106\ x_1{*}x_3 - 0.0241\ x_2{*}x_3 + d_6^+ - d_6^- = 3 \quad (7)$$

Subject to

$$500 \le x_1 \le 1000 \quad (8)$$

$20 \le x_2 \le 40$ (9)

$0 \le x_3 \le 1$ (10)

$d_i^+, \quad d_i^- \ge 0, \ i=1,\ldots 6.$

The GP model is solved using the Microsoft Excel's Solver Tool. The obtained optimal factor values are provided for different scenarios in Table 8. Optimal factor levels are x_1=500, x_2= 25.96, and x_3= 0.33, respectively. The preemptive goal programming methodology is used to solve the developed scenarios. In the scenarios, some responses are considered more important (critical) than the other(s). Table 8 and Figure 4 analysis shows that the tool rotation speed value does not change in different scenarios. However, the feed rate and the tool tilt angle factors' values change in the developed scenarios. An increase in the optimum feed rate reduces the optimum tool tilt angle, according to Figure 7. Based on these observations it can be concluded that the tool rotation speed can be kept constant at 500 rpm whereas the tool tilt angle must be reduced when the feed rate should be increased to lower the welding time.

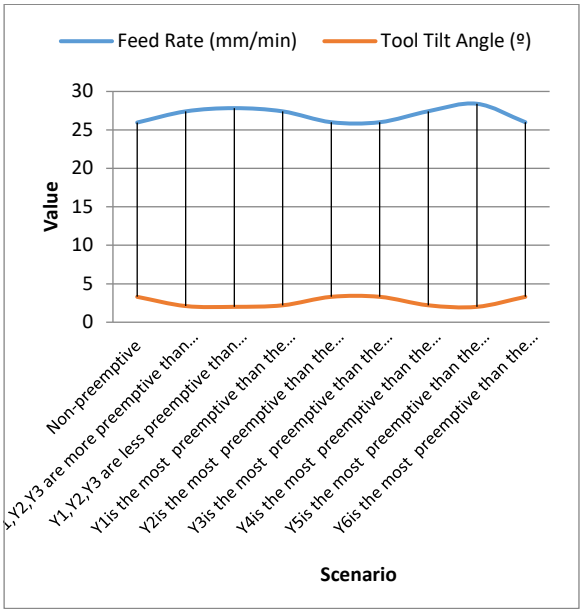

Fig. 4. Scenario analysis results (see Table 8).

Effects of Process Parameters on Tensile Strength

The welded samples are first subjected to the tensile test. Figure 5a provides the average tensile strength for each combination of the two aluminum types. As can be seen from the graphic, especially the AA7075-AA7075 pair showed a very brittle fracture behavior. The AA6061-AA7075 material pair showed almost the same strength as the expected value but gave a higher elongation value as a result of the optimization. Compared to the others, a rather ductile rupture occurred in the AA6061-AA6061 material pair. However, considering that the AA6061-T6 material shows approximately 15% elongation ductility, it is clear that the FSW process causes crucial reductions in the material ductility (Figure 5a).

Effects of Process Parameters on Hardness

In both AA6061-AA6061 plate pairs and AA7075-AA7075 plate pairs, it is observed that as the distance from the advancing line, which is the weld center, increased up to 5 mm, the hardness increased and then decreased again along with the distance to the tool shoulder line. When the amount of softening that occurred in the tool shoulder line was analyzed, it is determined that softening of approximately 50% occurred in the AA6061-AA6061 combinations and AA6061-AA7075 combinations, while the softening rate was lower in the AA7075-AA7075 combinations (Figure 5b).

Effects of Process Parameters on Flexural Strength

According to the bending test results, the bending strength of AA6061-T6 aluminum alloy is calculated as 641.12 MPa, and the bending strength of AA7075-T6 aluminum alloy is obtained as 1235.98 MPa. The flexural strength values of the plates were similar to the characteristic properties of base metals. A more brittle fracture is observed in the sample of the AA7075–AA7075 plate pair (Figure 5c) because the AA7075-T6 aluminum alloy has a more brittle structure compared to the AA6061-T6 aluminum alloy.

Effects of Process Parameters on Macro and Microstructure

In the macro images of the AA6061-AA6061 plate pairs seen in Figure 6, the structure in the weld center is visible. The cracks in the root of the welded zone may have resulted due to the temperature differences between the work table and material. Figure 6 shows micrographs of the friction stir weld. Some researchers refer that friction stir welding is acquired by shear stress caused by the motion of the tool-pin surface. If shear stress occurs around the first butt surfaces when the friction stirs the welding process, the Al_2O_3 oxide layer can be broken down. Peel et al. (2003) recommended that slower movement speeds can eliminate the kissing surface. However, manufacturers may want to conduct high-speed friction stir welding to achieve the highest productivity. Therefore, the characteristics of welds with kissing bonds are needed to increase confidence in the design and implementation of FSW joints. We can say that the kissing bond is different from root defects. We can see from Figure 6 that the kissing bond is a weak line visible only in the mixing region (Figure 6a), and the root defect looks like a crack in the root portion of the FS welds (Figure 6b). Figure 7 shows kissing surfaces, another defect that can be encountered in friction stir welding. This error occurs on two surfaces in contact where complete coupling does not occur due to insufficient heat input. This situation, which occurs at

a heat input sufficient to cause plastic deformation of the materials but insufficient for their mixing, directly affects the mechanical properties of the welded sample. On the weld root of another sample of the AA6061–AA6061 plate pair, kissing surfaces are observed because of insufficient heat input (Figure 7). Since this defect is not seen again in other images taken from the weld section at points away from the welding start point, it is concluded that the existence of the insufficient initial waiting time at the welding start point might cause such microstructure defects. The zigzag lines were found in the AA6061–AA6061 plate joint in our results (Figure 7). In the literature, Liu (2013) stated that the zigzag line (ZZL) is the residual oxide layer in FSW joints because of the inadequate heat input. We can say that the existence of the zigzag in the weld zone deteriorates the tensile strength of the heat-treated joints (Figure 7). As stated by Sato et al.'s (2004) study in the advancing side-welded situation, the ZZL is included in broken oxide particles. In summary, the ZZL affects the tensile specifications of the heat-treated joints. So, surface preparation before the process is crucial to avoid the existence of the ZZL in the welded joint to set high-quality parts. In FSW, more heat is released from the retraction side on the advancing side (Sahu 2021). Since the melting point temperature of AA6061 is higher than the AA7075 aluminum alloy, it is positioned on the advancing side during the joining processes. Correspondingly, as observed in Figure 8 b, a larger heat-affected surface formation on the AA7075 side was seen. On the other hand, in the AA6061–AA7075 combination, the thermo-mechanically affected region on the retraction side covers a larger area (Figure 8. a). Figure 8 shows that only AA7075 material is mixed into AA6061 depending on the melting point temperature difference. On the other hand, it is seen that the penetration of AA6061 material into AA7075 material is very limited (Figure 8 b). Based on this, it is thought that the friction stir welding tool with flat cylindrical geometry may have been insufficient at the point of material transition. In the AA6061–AA7075 plate pairs, as in the AA6061-AA6061 plate pairs, the images were taken on the cross-sections on kissing surfaces (Figure 9 a). It is seen that the input heat was sufficient. Therefore, no kissing surfaces were formed. So, a full surface weldment was achieved (Figure 9 b). In the images taken from the AA6061–AA7075 plate surface, groove formations containing intermittent spaces formed on the surface were observed (Figure 10a). In addition, it was observed that the amount of thinning in the weld area was higher, especially on the AA7075 side (Figure 10b). In Figure 11, in the AA7075-AA7075 pair, it has been observed that many micro-sized voids are formed in the internal structure. These micro-sized voids are less common in the dynamically recrystallized region.

CONCLUSIONS AND RECOMMENDATIONS

At the end of the study, it can be concluded that the maximum tensile strength and elongation amounts obtained from the materials increase as the tool tilt angle approaches 1°, the highest value used in the experiments. However, it can also be said that increasing the tool tilt angle too much will reduce the contact on the advanced side of the tool so that the total force on the pin will increase and damage the tool.

Many defects observed in friction stir welding, such as micro-cracks, micro-tunnels, micro-voids, and lack of penetration, can be prevented using preventive measures such as preheating. Although recrystallization is rare in aluminum materials, it is observed that especially in the AA7075–AA7075 aluminum plate pair, recrystallization occurred in the welding centers, and a finer grain structure was obtained. In addition, because of insufficient heating, various microstructure defects are observed in the internal structure images taken from places close to the weld starting point. Most defects are not seen in the images taken from farther points. Experimental results for the average tensile strength values graph are shown in Figure 12. It can be easily seen that the AA6061-AA6061 combinations have the lowest tensile strength values. On the other hand, AA6061-AA7075 combinations have the best tensile strength values considering the experimental results (Table 5). However, the maximum elongations occurred with the AA6061-AA6061 combinations (Figure 13). Optimal parameters for all Y responses were obtained at 500 rpm rotation speed, 25.96 mm/min feed rate, and 0.33° tool tilt angle.

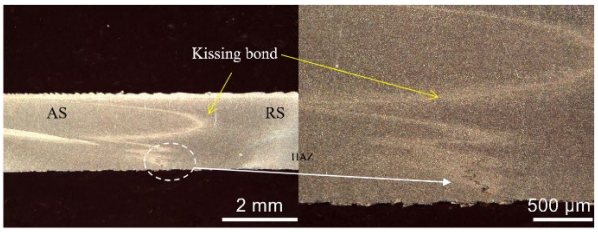

Fig. 6. Crack in the weld root of the weldments of the AA6061–AA6061 plates.

For dissimilar combination (AA6061-AA7075) joining, we obtained the optimal parameter values at 500 rpm rotation speed, 26 mm/min feed rate, and 0.33° tool tilt angle in the Y2 is more critical than the other scenario (Table 7) for the best tensile strength.

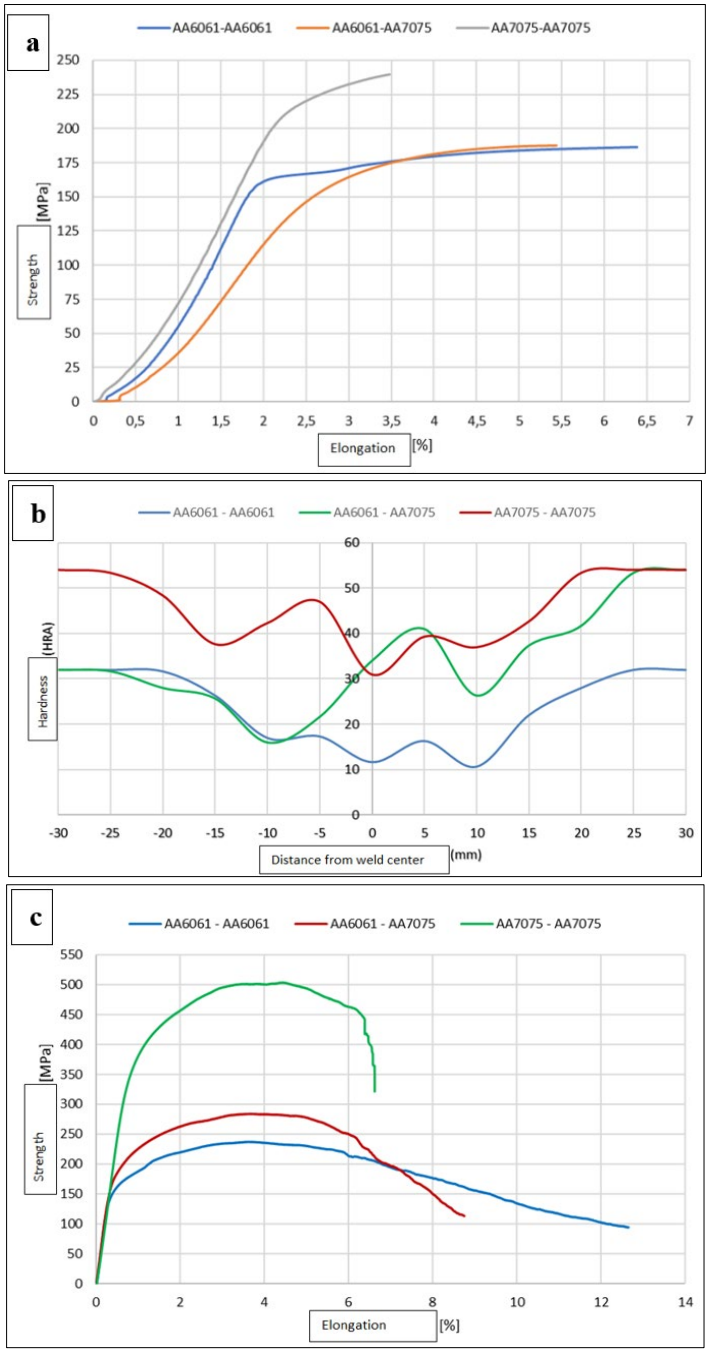

Fig. 5. Results of the experiments.

Table 7. Regression functions for the two responses (yield strength; elongation).

Tensile Strength (MPa)	$\sigma_{max}AA6061-AA6061$	155.2 – 0.2170 x_1+ 4.77 x_2 – 12.1 x_3 + 0.000149 x_1^2- 0.0857 x_2^2 + 5.82 x_3^2 + 0.000068 x_1*x_2 – 0.0215 x_1*x_3+ 1.511 x_2*x_3	R-sq(adj): 90.20	Explanation
	$\sigma_{max}AA6061-AA7075$	177.9 – 0.2048 x_1+ 4.55 x_2 – 27.4 x_3 + 0.000149 x_1^2- 0.0857 x_2^2 + 5.82 x_3^2 + 0.000068 x_1*x_2 – 0.0215 x_1*x_3+ 1.511 x_2*x_3	92.51	x_1: Spindle Speed x_2: Feed Rate x_3: Tool Angle
	$\sigma_{max}AA7075-AA7075$	167.4 – 0.2837 x_1+ 9.32 x_2 – 23.6 x_3 + 0.000244 x_1^2- 0.1469 x_2^2 – 16.72 x_3^2 – 0.001651 x_1*x_2 – 0.0258 x_1*x_3+ 1.952 x_2*x_3	94.15	
Elongation (%)	$\sigma_{max}AA6061-AA6061$	6.25 + 0.0055 x_1 – 0.24 x_2 + 3.22 x_3 + 0.000149 x_1^2+ 0.00703 x_2^2 + 1.19 x_3^2 – 0.000231 x_1*x_2 – 0.00261 x_1*x_3- 0.0744 x_2*x_3	87.57	
	$\sigma_{max}AA6061-AA7075$	+1.29 + 0.01171 x_1+ 0.049 x_2 + 1.79 x_3 – 0.000007 x_1^2+ 0.00001 x_2^2 + 0.29 x_3^2 – 0.000006 x_1*x_2 – 0.00212 x_1*x_3- 0.0121 x_2*x_3	88.9	

	$\sigma_{max}AA7075 - AA7075$	-4.47 + 0.0182 x_1+ 0.001 x_2 – 0.17 x_3 – 0.000012 x_1^2- 0.00011 x_2^2 + 0.773 x_3^2 + 0.000007 x_1*x_2 + 0.00106 x_1*x_3- 0.0241 x_2*x_3	81.47	

Table 8. Optimum process parameters.

Goal Programming Scenarios	Optimum parameter values			Results					
	Tool Rotation Speed (rpm)	Feed Rate (mm/min)	Tool Tilt Angle (°)	Y1	Y2	Y3	Y4	Y5	Y6
Non-preemptive (original)	500	25.96	0.33	156.34	174.84	210.82	41.86	5.69	1.60
Y1-Y3 are more critical than Y4-Y6	500	27.41	0.21	155.40	174.95	211.85	41.81	5.61	1.61
Y1-Y3 are less critical than Y4-Y6	500	27.83	0.20	155.34	174.96	212.07	41.82	5.61	1.61
Y1 is more critical than the others	500	27.41	0.22	155.61	175.01	211.95	41.82	5.62	1.61
Y2 is more critical than the others	500	26	0.33	156.98	175.01	210.98	41.88	5.71	1.59
Y3 is more critical than the others	500	26	0.33	156.98	175.01	210.98	41.88	5.71	1.59
Y4 is more critical than the others	500	27.43	0.22	155.62	175.01	211.97	41.82	5.62	1.61
Y5 is more critical than the others	500	28.4	0.20	155.51	175.00	212.43	41.83	5.61	1.61
Y6 is more critical than the others	500	26	0.33	156.98	175.01	210.98	41.88	5.71	1.59

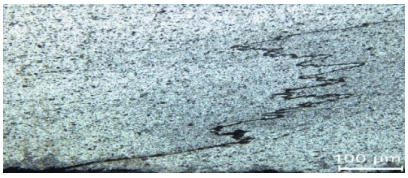

Fig. 7. Kissing surfaces at the weld root in the weldment of the AA6061–AA6061 plates.

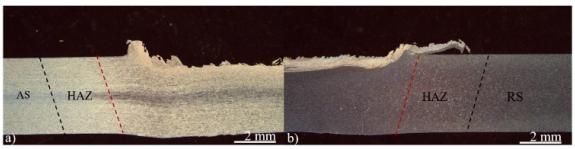

Fig. 8. Additional surfaces formed in the welded AA6061–AA7075 plates a) shown on the AA6061 b) shown on the AA7075.

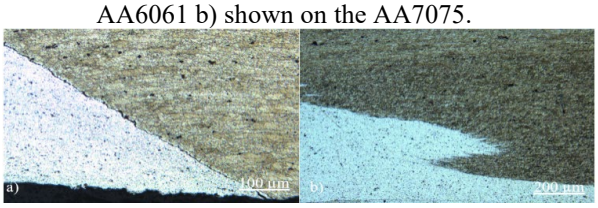

Fig. 9. Kissing surfaces formed because of the lack of fusion in the welded AA6061–AA7075 plates a) Distance from starting edge = 20 mm, b) Distance from starting edge= 40 mm.

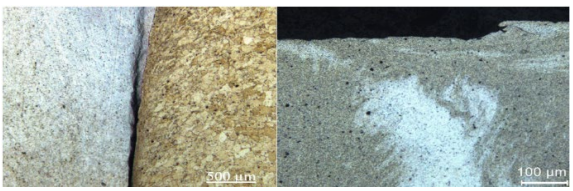

Fig. 10. Groove formation and section thinning in the welded AA6061–AA7075 plates: Left) Weld surface, Right) Weld section.

On the other hand, we determined the optimal parameter values for the dissimilar combination's elongation (Y5 is more critical than the others) at 500 rpm rotation speed, 28.4 mm/min feed rate, and 0.20° tool tilt angle.

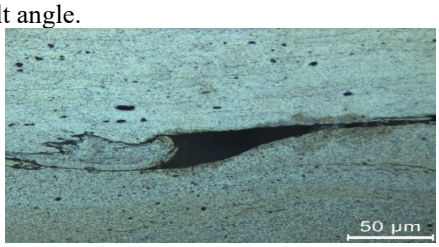

Fig. 11. Micro tunnel formation in the weldment of AA7075–AA7075 plates.

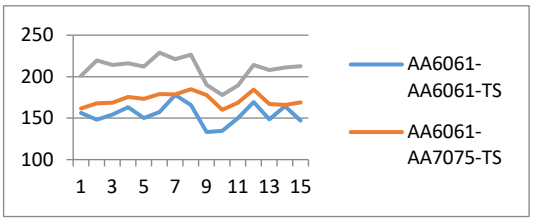

Fig. 12. Graphical illustration for experiment result of tensile strength.

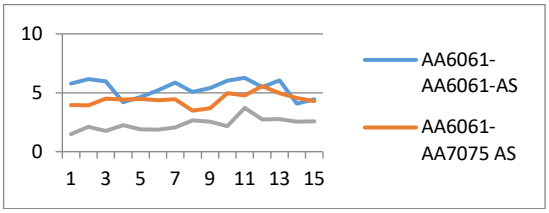

Fig. 13. Graphical illustration for experiment result of elongation.

REFERENCES

Balamurugan, S., Jayakumar, K., Subbaiah, K., "Influence of Friction Stir Welding Parameters on Dissimilar Joints AA6061-T6 and AA5052-H32," *Arab J Sci Eng.,* Vol.46 No.12 pp.11985-11998 (2021).

Banik, A., Saha, A., Barma, J. D., Acharya, U., & Saha, S. C., "Determination of best tool geometry for friction stir welding of AA 6061-T6 using hybrid PCA-TOPSIS optimization method," *Measurement* Vol. 173 No. 108573 (2021).

Chowdhury, I., Sengupta, K., Maji, K. K., Roy, S., & Ghosal, S., "Investigation of mechanical properties of dissimilar joint of Al6063 aluminium alloy and C26000 copper alloy by ultrasonic assisted friction stir welding," *Materials Today: Proceedings*, Vol.50, pp.1527-1534 (2022).

Fathi, J., Ebrahimzadeh, P., Farasati, R., & Teimouri, R., "Friction stir welding of aluminum 6061-T6 in presence of watercooling: Analyzing mechanical properties and residual stress distribution," *International Journal of Lightweight Materials and Manufacture* Vol. 2 No.2 pp. 107-115 (2019).

Ghiasvand, A., Hassanifard, S., Jalilian, M. M., Kheradmandan, H., "Investigation of tool offset on mechanical properties of dissimilar AA6061-T6 and AA7075-T6 joint in parallel FSW process," *Welding in the World* Vol. 65 pp. 441-450 (2021).

Gill, A., Dhiman, D. P., Gulati, V., Sharma, S., "Mathematical modeling of process parameters of friction stir welded aluminium alloy joints using central composite design," Materials Today: Proceedings Vol. 5 No.14 pp. 27865-27876 (2018).

Harisha, P., Nanjundaswamy, H. M., Divakar, H. N., & Krishnan, D., "Tensile properties of aluminium and copper alloys friction stir welded joints," *Materials Today: Proceedings, Vol.*54, pp.223-227 (2022).

Jia, H., Wu, K., Sun, Y. et al., "Experimental research and process parameter optimization of high-speed friction stir welding," *Int J Adv Manuf Technol.,* Vol. 115 pp.3829–3838(2021).

Khan, N., "Optimization of Friction Stir Welding of AA6062-T6 Alloy," *Materials Today: Proceedings* Vol.29 pp. 448-455 (2020).

Kumar, R., Dhami, S.S., Mishra, R., "Optimization of friction stir welding process parameters during joining of aluminum alloys of AA6061 and AA6082," *Materials Today: Proceedings* Vol. 45 pp.5368-5376 (2021).

Liu, H., Hou, J., Guo, H., "Effect of welding speed on microstructure and mechanical properties of self-reacting friction stir welded 6061-T6 aluminum alloy," *Materials & Design* Vol. 50 pp. 872-878 (2013).

Maneiah, D., Mishra, D., Rao, K. P., & Raju, K. B., "Process parameters optimization of friction stir welding for optimum tensile strength in Al 6061-T6 alloy butt welded joints," *Materials Today: Proceedings* Vol. 27 pp. 904-908 (2020).

MirHashemi, S., Amadeh, A., and Khodabakhshi, F., "Effects of SiC nanoparticles on the dissimilar friction stir weldability of low-density polyethylene (LDPE) and AA7075 aluminum alloy," *Journal of Materials Research and Technology,* Vol. 13, pp. 449-462 (2021).

Mohamed, M. F., Yaknesh, S., Kumar, C. A., Rajadurai, J. G., Janarthanan, S., & Vignes, A. V. S., "Optimization of friction stir welding parameters for enhancing welded joints strength using Taguchi based grey relational analysis," *Materials Today: Proceedings* Vol.39 pp. 676-681 (2021).

Moradi, M. M., Aval, H. J., Jamaati, R., Amirkhanlou, S., & Ji, S., "Effect of SiC nanoparticles on the microstructure and texture of friction stir welded AA2024/AA6061," *Materials Characterization* Vol. 152 pp. 169-179 (2019).

Peel, M., Steuwer, A., Preuss, M., Withers, P.J., "Microstructure, mechanical properties and residual stresses as a function of welding speed in aluminium AA5083 friction stir welds," *Acta Mater* Vol.51 No.16 pp. 4791-4801 (2003).

Pitchipoo, P., Muthiah, A., Jeyakumar, K., & Manikandan, A., "Friction stir welding parameter optimization using novel multi objective dragonfly algorithm," International Journal of Lightweight Materials and Manufacture Vol. 4 No.4 pp. 460-467 (2021).

Prabhu, S.R., Shettigar, A., Herbert, M.A. et al., "Parameter investigation and optimization of friction stir welded AA6061/TiO2 composites through TLBO," Weld World Vol.66 No.1 pp. 93-103(2021).

Rahmatian, B., Dehghani, K., Mirsalehi, S.E., "Effect of adding SiC nanoparticles to nugget zone of thick AA5083 aluminium alloy joined by using double-sided friction stir welding," *Journal of Manufacturing Processes*, Vol.52, pp. 152-164 (2020).

Rzaev, R., Dzhalmukhambetov, A., Chularis, A., Valisheva, A., "Mathematical modeling of process of the friction stir welding," *Materials today: proceedings* Vol. 11pp.591-599 (2019).

Sahu, M., Paul, A., and Ganguly, S., "Optimization of process parameters of friction stir welded joints of marine grade AA 5083," *Materials Today: Proceedings* Vol.44, pp. 2957-2962 (2022).

Sandeep, R., Jeevanantham, A. K., Manikandan, M., Arivazhagan, N., Tofil, S., "Multi-Performance Optimization in Friction Stir Welding of AA6082/B 4 C Using Genetic Algorithm and Desirability Function Approach for Aircraft Wing Structures," Journal of Materials Engineering and Performance Vol.30 No.8 pp. 5875-5857 (2021).

Sato, Y. S., Yamashita, F., Sugiura, Y., Park, S. H. C., Kokawa, H., "FIB-assisted TEM study of an oxide array in the root of a friction stir welded

aluminium alloy," *Scripta materialia*, Vol. 50 No.3 pp. 365-369 (2004).

Shekar, K.C. and Kumar, S.S., "A review on ultrasonic characterisation of dissimilar plates by friction stir welding," *Materials Today: Proceedings* Vol.51, pp.1021-1025(2022).

Shunmugasundaram, M., Kumar, A. P., Sankar, L. P., & Sivasankar, S., "Optimization of process parameters of friction stir welded dissimilar AA6063 and AA5052 aluminum alloys by Taguchi technique," *Materials Today: Proceedings* Vol. 27pp. 871-876 (2020).

Singh, T., "Processing of friction stir welded AA6061-T6 joints reinforced with nanoparticles," *Results in Materials*, Vol.12, No. 100210 (2021).

Sun, Y., and Fujii, H., "Improved resistance to hydrogen embrittlement of friction stir welded high carbon steel plates," *International Journal of Hydrogen Energy*, Vol. 40 No.25, pp. 8219-8229 (2015).

Thilagham, K., Muthukumaran, S., "Process parameter optimization and characterization of friction stir welded advancing side AA6082-T6 with retreating side AA7075-T651," *Materials Today: Proceedings* Vol. 27 pp. 2260-2264 (2020).

Umanath, K., Palanikumar, K., Sankaradass, V., & Uma, K., "Optimizations of friction stir welding process parameters of AA6063 aluminium alloy by Taguchi technique," *Materials Today: Proceedings,* Vol.46 pp.4008-4013 (2021).

Verma, S., Kumar, V., "Optimization of friction stir welding parameters of dissimilar aluminium alloys 6061 and 5083 by using response surface methodology," *Proceedings of the Institution of Mechanical Engineers, Part C: Journal of Mechanical Engineering Science* Vol.235 pp.7009-7020 (2021).

Wu, D., Li, W., Liu, X., Gao, Y., Wen, Q., & Vairis, A., "Effect of material configuration and welding parameter on weld formability and mechanical properties of bobbin tool friction stir welded Al-Cu and Al-Mg aluminum alloys," *Materials Characterization,* Vol. 182, No. 111518 (2021).

Yaghoubi, S. and Shirazi, A., "Mechanical properties and corrosion behavior of friction stir welded copper plates under shielding gas," *International Journal of Fatigue* Vol. 152, No. 106419 (2021).

Yurdakul, M., Tukel, T., and İç, Y.T., "Development of a Goal Programming Model Based on Response Surface and Analytic Hierarchy Process Approaches for Laser Cutting Process Optimization of St-52 Steel Plates," *Journal of Advanced Manufacturing Systems* Vol. 21, No. 02, pp. 293-316 (2022).